Application of Schottky barrier bolometer arrays to cooled sensors

Freeman D. Shepherd and James E. Murguia

Solid State Scientific Corporation

27-2 Wright Road

Hollis, New Hampshire 03049

ABSTRACT

We describe a model for cooled thermal imaging sensors, based on silicon Schottky diode bolometer arrays. The sensing mechanism is the modulation of Schottky diode dark current with temperature. The proposed array is identical to Schottky diode arrays, which would be used for uncooled thermal imaging, except for a change of the sensing electrode metal. We separate the thermal and electrical response of the detector elements and discuss sensor limitations related to detector thermal isolation. At a 180 K operating temperature, we project NEDT's in the 3 to 20 mK range, depending upon system f/number. A 20 cm aperture sensor based on this technology should have a noise equivalent power below 10^{-11} watts.

Keywords: Cooled sensors, Infrared imaging, Bolometer arrays, Thermionic emission

1. INTRODUCTION

This paper describes a theoretical model for predicting the performance of infrared staring mode sensors, based on Schottky barrier bolometer arrays. The infrared detectors are metal-silicide / silicon Schottky junctions that are integral to the focal plane chip. The detector elements are thermally isolated, using directional etching and other techniques, which have been developed for fabrication of silicon micro-mechanical devices (MEMs). When an infrared image is incident on the array, the temperature of individual diodes rises in proportion to the local image power. The temperature rise causes an increase in diode saturation current, resulting in an electronic image output from the array. We describe this sensing mechanism and project expected noise equivalent temperature difference (NETD) and noise equivalent power (NEP) for example sensors based on this technology. Similar models, which were developed earlier to describe the performance of Schottky diode photo-emissive sensors, predicted performance to within a few percent of experimental observation. Similar results are expected for the current analysis, because, except for thermal isolation, the arrays are quite similar to current metal-silicide arrays. The sensing current in the bolometer arrays is the Richardson "dark current" found in photo-emissive arrays.

2. THE BOLOMETER ARRAY THERMAL RESPONSE

Localized power from a remote source, or image, is incident on a sensing element in the array, causing a rise in the element temperature. We measure the temperature rise by observing the change of some temperature dependent property of the sensing element. Detector optimization becomes a two-step process, maximization of sensing element temperature change with incident power and optimization of the temperature sensing response mechanism. This is continued until the measurement is limited by system considerations, or by thermal run away.[1] The end goal is to reach an operating mode wherein the dominant noise in the measurement is thermal fluctuation noise, or ultimately, radiation noise from detector thermal emission to the surround.

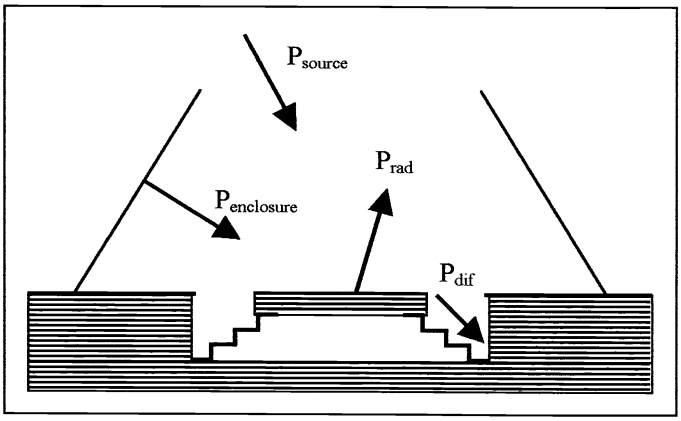

Figure 1. Schematic of power balance at sensing element

Infrared Technology and Applications XXVI, Bjørn F. Andresen, Gabor F. Fulop, Marija Strojnik, Editors,
Proceedings of SPIE Vol. 4130 (2000) © 2000 SPIE. · 0277-786X/00/$15.00

Today, all competitive bolometer array devices are manufactured as silicon integrated circuits, where MEMs processing technique are employed to form detector thermal isolation structures. The thermal balance for a detector element is shown schematically in Figure1. The detector element is illuminated by radiation from the sensor optical aperture and from the surrounding enclosure, or cold shield. The detector radiates to its surround and conducts heat to the focal plane substrate, through its support structure. The latter conduction mechanism tends to clamp the detector temperature to the substrate. As a result, the detector temperature will always be close to the sensor enclosure temperature.

Consider the case of incident radiation from a blackbody source of arbitrary temperature, T_s. The detector power balance is given by Equation 1.[2]

$$A_d\varepsilon_d\sigma T_d^4 + G_{dif}(T_d - T_e) = \frac{A_d\varepsilon_d\sigma T_s^4}{4F^2+1} + \left(1 - \frac{1}{4F^2+1}\right)A_d\varepsilon_d\sigma T_e^4 \tag{1}$$

where A_d, ε_d and T_d are the active area, emissivity and temperature of the detector, σ is the Stephan-Boltzmann constant, T_e the sensor enclosure temperature, F the sensor f/number and G_{dif} the detector thermal conductance to the substrate.

We apply a binomial expansion about T_e noting that the detector radiative conductance G_{rad} is given by:

$$G_{rad} = 4A_d\varepsilon_d\sigma T_d^3. \tag{2}$$

Then if T_s is approximately equal to T_e, as is the case for uncooled thermal imaging sensors, the temperature change of the detecting element will be given by:

$$\Delta T_d = \left(\frac{1}{4F^2+1}\right)\frac{G_{rad}[\Gamma(T_s,\lambda_1,\lambda_2)]R(\tau_{th})}{G_{rad}+G_{dif}}\Delta T_s \tag{3}$$

where:

$$\Delta T_d = T_d - T_e \tag{4}$$

and

$$\Delta T_s = T_s - T_e \tag{5}$$

and

$$R(\tau_{th}) = 1 - \exp(-t_{fr}/\tau_{th}) \tag{6}$$

Equation 6 represents the signal roll off imposed by the detector thermal time constant τ_{th}, when the sensor operates with a frame time t_{fr}. Using C_{therm} as the thermal capacitance of the detecting element, the thermal time constant is given by:

$$\tau_{th} = C_{therm}/(G_{rad}+G_{dif}) \tag{7}$$

The black body radiant power passed by the sensor optical band-pass filter, between wavelengths λ_1 and λ_2, is given by:

$$\Gamma(T_s,\lambda_1,\lambda_2) = \frac{\int_{\lambda_1}^{\lambda_2} W_\lambda(\lambda,T_s)d\lambda}{\sigma T_s^4} \tag{8}$$

where:

$$W_\lambda(\lambda,T_s) = \frac{2\pi hc^2}{\lambda^5\left(\exp\left(\frac{hc}{\lambda kT_s}\right)-1\right)} \tag{9}$$

is the spectral radiant emittance, h Planck's constant, k Boltzmann's constant and c the velocity of light.[3]

When ΔT_s is large, as is the case for a cooled thermal imaging sensor, Equation 3 can be generalized by including all terms in T_s from the binomial expansion of Equation 1, resulting in Equation 10. Note that our sensor is identical to sensors, which have been proposed for uncooled thermal imaging. Only the Schottky barrier material and the related barrier potential have been changed to accommodate cooled operation

$$\Delta T_d = \left(\frac{1}{4F^2+1}\right)\frac{G_{rad}(1+\xi(\Delta T_s))[\Gamma(T_s,\lambda_1,\lambda_2)]R(\tau_{th})}{G_{rad}+G_{dif}}\Delta T_s \tag{10}$$

$$\Delta T_d = H(T_s)\Delta T_s \tag{10a}$$

where

$$\xi(\Delta T_s) = 6\left(\frac{\Delta T_s}{T_e}\right)^2 - 4\left(\frac{\Delta T_s}{T_e}\right)^3 + \left(\frac{\Delta T_s}{T_e}\right)^4 \tag{11}$$

Equation 10 gives the detector large-scale signal response. The term $H(T_s)$ given in Equation 10a is the static thermal transfer response for the detecting element. This equation is used to determine the temperature offset imposed on a cooled detector by the ambient background. It is also used to determine the differences in signals from sources having distinct temperatures. We applied Equation 10 to determine the detector temperature offset as a function of the cooling temperature ΔT_s. The result is given in Figure 2. The detector temperature offset is less than one percent of the cooling temperature difference between the sensor enclosure and the observed scene. This is consistent with the thermal transfer response, or gain, $H(T_s)$. As detector thermal conduction losses are reduced, the thermal transfer gain will improve.

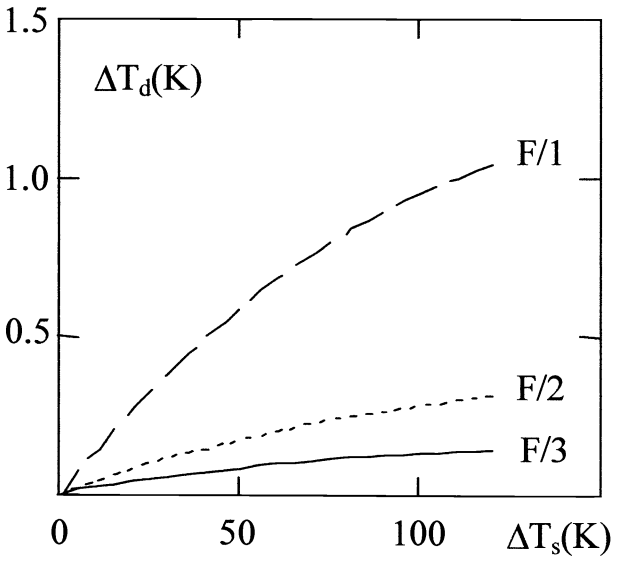

Figure 2 Detector temperature rise ΔT_s above enclosure as a function of cooling temperature.

The small-scale signal response of the sensing element was determined by considering a temperature difference of 1K at T_s, resulting in:

$$\Delta T_{dt} = \Delta T_d(T_s+1) - \Delta T_d(T_s) \tag{12}$$

$$\Delta T_{dt} = h(T_s)\delta T_s(T_s) \tag{12a}$$

Equation 12 was employed to determine the incremental detector temperature change ΔT_{dt} as a function a small change of temperature in the observed scene δT_s. It is this temperature difference that will be measured to characterize, or detect, object detail in the observed scene. Equation 12a gives the sensor incremental transfer gain. In Figure 3, we compare the incremental response for f/2 and f/3 sensors. Note that cooling the sensor enclosure by 100K results in less than 3 percent increase in the detector temperature response to the test source. As detector thermal isolation techniques improve, the absolute differential response will also increase, but the change in response with cooling temperature will still be small.

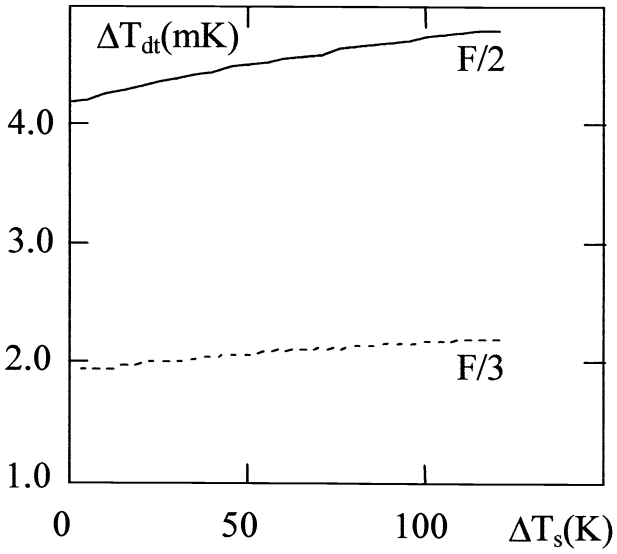

Figure 3 Detector temperature difference for 1K test source at 290 K vs. sensor cooling temperature.

The principle factor limiting the sensitivity of bolometer arrays is conduction loss to the focal plane substrate. We have noted that this conduction clamps the detector element temperature. Values of thermal conductance G_{dif}, for current art uncooled detector arrays, are near 50 nwatt/K. In Figure 4, we give the incremental thermal response as a function of detector cooling, with thermal conductance, G_{dif}, as a parameter. If, through improved detector cell design, thermal conductance losses can be reduced 10-fold, the detector incremental response will double. The same increase will be observed in the detector electrical responsivity.

In our computation we selected a detector thickness of 0.65 um, which gives resonant power absorption in the silicon based detector element. This selection results in a relatively high thermal capacitance and a reduction in sensor incremental temperature response. In Figure 5, we indicate the improvement in incremental response, which might be obtained by reducing detector thickness. Reducing thermal capacitance results in an equal reduction in detector thermal time constant. Reducing thermal capacitance will not improve the response, if the sensor is not thermal bandwidth limited.

3. SCHOTTKY DIODE ELECTRICAL RESPONSE AND NOISE

Thermionic emission within the Schottky diode is used to observe the temperature change of the sensing element. Under

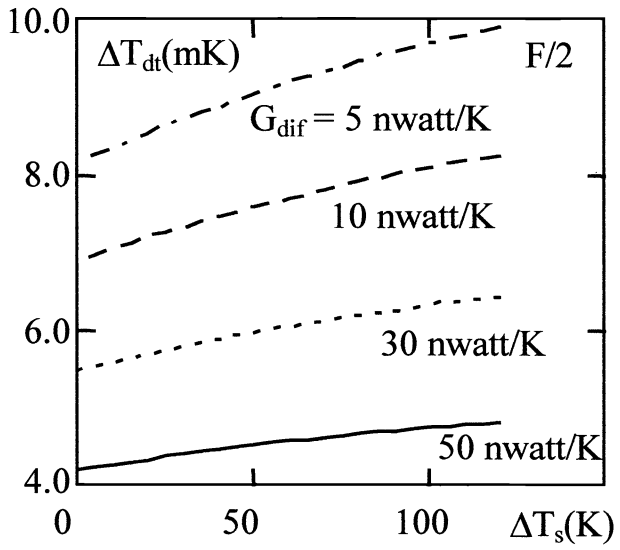

Figure 4 Incremental response vs. cooling, showing effect of G_{dif} as a parameter. Current detectors correspond to 50 nwatt/K curve.

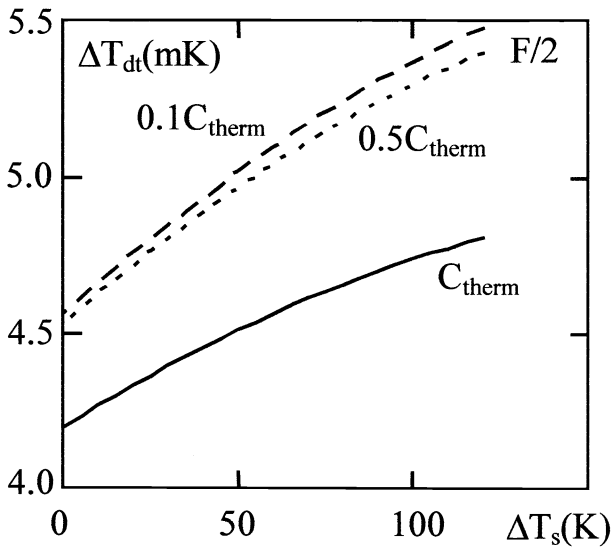

Figure 5. Demonstrates the potential for increasing the thermal response by increasing detector element thermal bandwidth, through reduction in mass.

reverse bias, Schottky diode saturation current density is dominated by thermionic emission, given by the Richardson equation:

$$J_s = A_r T_d^2 \exp(-\Phi_{bn} / kT_d) \tag{13}$$

Where A_r is Richardson's constant, k is Boltzmann's constant, T_d the absolute temperature of the detecting element and Φ_{bn} the Schottky barrier potential at the operating bias voltage. The value of Φ_{bn} is determined by an activation energy analysis of the variation of diode current with temperature. The Richardson constant for p-type silicon Schottky barriers is 30 amperes/cm^2/K^2.

The Schottky diode current-voltage response is given by:

$$I_d = A_e J_s (e^{qV/kT} - 1) \tag{14}$$

When the detector is operated under reverse bias, at voltages large compared to kT/q, the reverse diode current reduces to the saturation current.

$$I_d = A_e J_s \tag{15}$$

The resulting temperature coefficient for thermionic emission, α_T, is given by:

$$\alpha_T = \frac{1}{J_R}\frac{\partial J_R}{\partial T} = \frac{1}{T}\left(\frac{q\Phi_{bn}}{kT} + 2\right). \tag{16}$$

The mean square shot noise in the emission current is given by,

$$< i_{Shot}^2 >= 2qB_e A_e A_r T_d^2 \, e^{\frac{-q\phi_{bn}}{kT}} \tag{17}$$

where B_e is the electrical bandwidth of the detector read-out network. Johnson noise is negligible in the measurement.[4]

The detector output amplifier contributes additional noise:

$$< i_{amp}^2 >= 2v_{na}^2 \left(\frac{1}{R_f} + \frac{qA_e}{kT} J_s e^{qV/kT}\right)^2 \tag{18}$$

where v_{na} is the input referred voltage noise of the amplifier and R_f is the amplifier feedback resistance.

All of the above noise mechanisms are similar to mechanisms observed in photon detectors. Thermionic detectors will exhibit an additional noise, because of the low detector element mass. Thermal fluctuations in the detector will modulate the detector temperature and the related thermionic emission current. The contribution of thermal fluctuation noise to the mean square noise equivalent power (NEP) of the detector is given by:[5]

$$< NEP_{th} >^2 = 4kT^2 B_{th} G_{th} . \tag{19}$$

This noise will be observed as an additional electrical noise:

$$< i_{th}^2 >= \frac{4kT^2}{C_{th}}\left(\frac{\partial I_s}{\partial T}\right)^2 . \tag{20}$$

At any significant reverse bias above kT/q, the diode impedance becomes very large, so as to give a negligible contribution to the amplifier noise. Under these conditions the total mean square noise becomes:

$$< i_{tot}^2 >= 2qBA_e J_s + \frac{4kA_e^2 J_s^2}{C_{th}}\left(\frac{q\Phi_{bn}}{kT_b} + 2\right)^2 + 2\frac{v_{na}^2}{R_f^2} \tag{21}$$

4.0 NOISE EQUIVALENT TEMPERATURE / POWER

When a detector is illuminated by a source at ΔT_s, it will rise in temperature to ΔT_d, with a corresponding increase in diode current ΔI_d, given by:

$$\Delta I_d = I_d \alpha_T \Delta T_d = I_d \alpha_T H(T_s) \Delta T_s \tag{22}$$

and

$$\Delta I_{dt} = \alpha_T I_d \Delta T_{dt} \tag{23}$$

Note that α_T, the temperature coefficient for Schottky barrier thermionic emission, is a electrical property independent of the detector thermal design, and $H(T_s)$ is the sensor thermal transfer function, given by Equation 10a.

The signal to noise of this measurement is:

$$SNR = \frac{\Delta I_{dt}}{\sqrt{< i_{tot}^2 >}} \tag{24}$$

The Noise Equivalent Temperature is:

$$NEDT = \frac{\Delta T_{dt}}{SNR} = \frac{\sqrt{< i_{tot}^2 >}}{I_d \alpha_T H(T_s)} \tag{25}$$

We also consider point source detection. It is assumed that the sensor will respond to a full ambient background signal, which is not obscured by the point source. For this case, a point source term is added to the power balance relationship of Equation 1. The signal power at the detecting element is given by:

$$\Delta P_{ps} = \varepsilon_{ps} A_{ps} \sigma T_{ps}^4 \left(\frac{d_a^2}{R_{ps}^2} \right) \tag{26}$$

where d_a is the sensor aperture diameter and ΔT_{ps}, R_{ps}, ε_{ps} and A_{ps} are the point source temperature difference, range, emissivity and area, respectively The background response and noise is derived from Equation 10 and the point source contribution is added as:

$$\Delta T_{dps} = \left(\frac{d_a^2}{4R_{ps}^2} \right) \frac{\varepsilon_{ps} A_{ps} G_{rad} (1 + \xi(\Delta T_{ps}))[\Gamma(T_{ps}, \lambda_1, \lambda_2)] R(\tau_{th})}{\varepsilon_d A_d (G_{rad} + G_{dif})} \Delta T_{ps} \tag{27}$$

Illumination by an unresolved point source will change the detector current by:

$$\Delta I_{dps} = I_d \alpha_T \Delta T_{dps} \tag{28}$$

This will result in a sensor signal to noise ratio for the point source:

$$SNR_{ps} = \Delta I_{dps} / \sqrt{< i_{tot}^2 >} \tag{29}$$

corresponding to noise equivalent power:

$$NEP = P_{ps} / SNR_{ps} \tag{30}$$

5.0 PROJECTED SENSOR PERFORMANCE

The above model was employed to predict the response parameters for a down looking sensor, having a 20 cm aperture and operating in a 1000 km orbit. The physical parameters of the sensor are given in Table 1. The 8 - 14 um, LWIR band was selected to allow thermal imaging at sea level. Estimation of imaging performance in other spectral bands can be obtained by changing the wavelength limits for the optical band-pass filter. In general, an atmospheric model should be added.

Table 1 PHYSICAL PARAMETERS FOR SENSOR MODEL

System		Detector		Sources	
Optical aperture	20 cm	Element	Schottky diode	Broad background	290 K
F/number	1, 2, 3	Pixel dimension	50 um x 50 um	Emissivity	0.9
Frame rate	10 Hz	Thickness	0.65 um		
Optical transmission	1.0	Fill factor	Thermal 0.96 Electrical 0.90	Unresolved "point" target	500 K
Spectral band	8 – 14 um	Barrier potential	0.24 eV	Area	100 m^2
Load resistance	$3x10^4$ ohm	Bias voltage	-5.0 volts	Emissivity	0.8
Operating temperature	180 K	Thermal loss	50 nwatt/K	Range	1000 Km

The expected sensor performance is summarized in Table 2. Our analysis predicts roughly equal noise contribution from thermal fluctuations and from the current sensing amplifiers. We have assumed a current mode amplifier similar to that suggested by Murguia, et al.[2] The present results indicate an alternative output amplifier design may improve performance.

The suggested design approaches thermal fluctuation noise limited performance, but is far from the thermal radiation limit. Thus cooling the sensor gives a somewhat limited improvement in sensitivity. No significant improvement in performance is expected as long as the detector temperature variation is clamped by thermal conduction. This suggests a need for new detecting element suspension techniques. Work in thermal isolation must also consider how to maintain sensor bandwidth. Possible approaches might include thermal reset or switching techniques.

Table 2 EXPECTED SENSOR PERFORMANCE

NEDT at F/1	2.6 mK	GSD = 250 m
NEDT at F/2	8.7 mK	GSD = 168 m
NEDT at F/3	18.7 mK	GSD = 84 m
Temperature Coefficient	7.7 %	
Diode signal level	159 uamp	
Noise level	0.5 namp	
NEP at F/3	$8x10^{-12}$ watt	
SNR for 500 K target	88:1	

Never the less, the potential sensitivities predicted by our analysis could be useful in a wide range of surveillance, Earth resource and weather monitoring measurements.

6. SUMMARY

We have described the potential performance for a space based sensor, which would employ a cooled bolometer array for sensing. A thermal analysis shows the expected response performance improvement for thermal detectors would be small compared to that of photon detectors. However, at 180 K, bolometer arrays can be expected to give useful thermal imaging and point source detection in the LWIR band, between 8 and 14 um. This

operating temperature should allow elimination of mechanical cooling systems, resulting in substantial improvements in the system simplicity and reliability of space based LWIR sensing systems.

We have considered the use of the thermionic emission "dark current" in metal-silicide Schottky barrier detectors for the thermal sensing mechanism in a bolometer array. Based upon our experience with Schottky diode photo-emissive arrays, the proposed sensor is expected to have excellent producibility and uniformity, negligible 1/f-noise and a two-fold improvement in thermal coefficients, relative to current technology. The predicted NEDT's suggest possible application to ocean current mapping and similar measurements, where detection of small temperature differences is important. A useful signal to noise ratio was obtained for an unresolved 500K target, which we considered to be representative of a burning building. Subject to consideration of clutter rejection, point target detection may also be a possible application for the proposed technology.

---

[1] P. W Kruse, L. D. McGlauchlin and R. B. McQuistan, Elements of Infrared Technology, John Wiley and Sons, New York, pp. 345-349, 1962.

[2] J. E. Murguia, P. K. Tedrow, F. D. Shepherd, D. Leahy, and M. M. Weeks, "Performance Analysis of a Thermionic Thermal Detector at 400K, 300K, and 200K", Proc. SPIE, Vol. 3698, Infrared Technology and Applications XXV, Eds. B. F. Andresen and M. S. Scholl, pp. 361-375, 1999.

[3] J. M. Lloyd, Thermal Imaging Systems, Plenum Press, New York and London, p.20, 1975.

[4] F. D. Shepherd and J. E. Murguia, "A comparison of infrared detection mechanisms in thermal-emissive vs. photo-emissive silicon Schottky barrier arrays", Proc. SPIE, Vol. 4028, Infrared Detectors and Focal Plane Arrays, Ed. E. L. Dereniak and R, E. Sampson, pp. , 2000.

[5] B. R. Johnson, P. W. Kruse, "Silicon Microstructure Super-conducting Microbolometer Infrared Arrays," Proc. SPIE 2020, Infrared Technology XIX, Eds. B. F. Andresen and F. D. Shepherd, pp. 2-11, 1993.